Insights into the structure and nanomechanics of the Quatsome membrane by force spectroscopy measurements and molecular simulations

Berta Gumí-Audenis[1,2,3,¶], Silvia Illa-Tuset[4], Natascia Grimaldi[4,5], Laia Pasquina-Lemonche[1,4,†], Lidia Ferrer-Tasies[5], Fausto Sanz[2,3,1], Jaume Veciana[3,4], Imma Ratera[3,4], Jordi Faraudo[4,] Nora Ventosa[3,4*] and Marina I. Giannotti[3,2,1*]*

1 Institute for Bioengineering of Catalonia (IBEC), The Barcelona Institute of Science and Technology (BIST), Barcelona, Spain

2 Departament de Ciència dels Materials i Química Física, Universitat de Barcelona, Barcelona, Spain

3 Centro de Investigación Biomédica en Red (CIBER), Madrid, Spain

4 Institut de Ciència de Materials de Barcelona (ICMAB-CSIC), Campus UAB, Cerdanyola del Vallès, Spain

5 Nanomol Technologies SL, Mòdul de Recerca B, Campus Universitari de Bellaterra, 08193, Cerdanyola del Vallès, Spain

KEYWORDS. Quatsome; membrane; AFM; force spectroscopy; nanomechanics; molecular dynamics; atomistic simulation; bilayer structure; nanovesicles

ABSTRACT

Quatsomes (QSs) are unilamellar nanovesicles constituted by quaternary ammonium surfactants and sterols in defined molar ratios. Unlike conventional liposomes, QS are stable upon long storage such as for several years, they show outstanding vesicle to vesicle homogeneity regarding size and lamellarity, and they have the structural and physicochemical requirements to be a potential platform for site specific delivery of hydrophilic and lipophilic molecules. Knowing in detail the structure and mechanical properties of the QS membrane is of great importance for the design of deformable and flexible nanovesicles alternatives, highly pursued in nanomedicine applications like the transdermal administration route. In this work, we report the first study on the detailed structure of the Cholesterol:CTAB QS membrane at the nanoscale, using atomic force microscopy (AFM) and spectroscopy (AFM-FS) under controlled liquid environment (ionic medium and temperature) to assess the topography of supported QS membranes (SQMs) and to evaluate the local membrane mechanics. We further perform molecular dynamics (MD) simulations to provide an atomistic interpretation of the obtained results. Our results are direct evidence of the bilayer nature of the QS membrane, with characteristics of a fluid-like membrane, compact and homogeneous in composition, and which structural and mechanical properties depend on the surrounding environment. We show how ions alter the lateral packing, modifying the membrane mechanics. We observe that according to the ionic environment and temperature, different domains may coexist in the QS membranes, ascribed to variations in molecular tilt angles. Our results indicate that QS membrane properties

may be easily tuned by altering the lateral interactions either with different environmental ions or counterions.

1. INTRODUCTION

The field of nanomedicine has grown rapidly in the recent years. Great efforts have been addressed towards new drug delivery systems that may improve the administration of drugs in a more effective and safe manner, increasing their solubility and stability, overcoming the anatomical and physiological barriers by targeting specific organs/tissues, reducing their quick clearance from the body and therefore, their side effects.[1, 2] Different types of nanoparticles are explored, including metal, organic and polymeric nanoparticles and liposomes.[3-6] Liposomes are molecular self-assembled lipid-based nanovesicles, undoubtedly one of the most promising supramolecular assemblies for nanomedicine due to their great versatility with respect to size, composition, surface characteristics and capacity for integrating and encapsulating bioactive molecules, both hydrophobic and/or hydrophilic. Their membranes can be efficiently functionalized with ligands with different hydrophobicity, and different targeting units like peptides, antibodies, etc. Moreover, liposomes are well recognized as pharmaceutical carriers because of their biocompatibility, biodegradability and low toxicity.[7, 8]

The physicochemical and mechanical properties of the nanoparticles are key as they may affect the interaction with cells and tissues, the endocytic pathway,[9] the drug permeability, and the deformability, which is essential for some applications, like skin penetration.[10] In lipid nanovesicles, the deformability and mechanical properties of the vesicles is directly related to the membrane structure and rigidity.[11, 12] The mechanical properties of the liposome membrane can be tuned by adjusting the membrane composition, including phospholipids in fluid or gel phase,

incorporating sterols, or adding sphingolipids or ceramide derivatives.[13-21] Among several attempts in this direction, are the novel generations of lipid vesicles, mainly flexible or elastic vesicles (transferosomes) and ultradeformable liposomes, that incorporate surfactants like edge activators to increase the elasticity of liposomes and lower their transition temperature (T_m).[8, 22-26]

Still, one of the major problems limiting the widespread use of liposomes is their poor stability, both physical (colloidal), including aggregation or fusion of vesicles to form larger and heterogeneous particles, and chemical, *i.e.* hydrolysis of ester groups and oxidation of unsaturated chains.[27] Liposomes with higher stability generally comprise gel phospholipids, and therefore deformability is compromised. The need for alternative vesicular systems with enhanced properties compared to liposomes, especially when vesicles' mechanical properties are a critical issue, has led to the design of alternative lipid nanovesicles, like the Quatsomes (QS). QS are unilamellar nanovesicles constituted by quaternary ammonium surfactants and sterols in defined molar ratios.[8, 28, 29] Unlike conventional liposomes, QS are stable upon long storage such as for several years, and they show outstanding vesicle to vesicle homogeneity regarding size and lamellarity.[29, 30] QS fulfill the structural and physicochemical requirements to be a potential encapsulation platform for site specific delivery of both hydrophilic and lipophilic molecules.[31-34] QS-like structures have been prepared using different quaternary ammonium surfactants such as cetrimonium bromide (CTAB), myristalkonium chloride (MKC) and cetylpyridinium chloride (CPC) and different sterols such as cholesterol (Chol) and b-sitosterol.[28, 29]

Using molecular dynamic (MD) simulations, it has been demonstrated that, in an aqueous environment, the synergy between the cetyltrymethyl ammonium (CTA^+) of CTAB and Chol molecules makes them self-assemble into bimolecular amphiphiles (synthon) and then into bilayers, with a similar structure of those formed by double-tailed unimolecular amphiphiles, like

phospholipids.[29] However, a detailed characterization on the structure and mechanical properties of the QS membrane has not been performed. Local characterization of these membrane properties can be widely explored with techniques that allow working at nanometric resolution and preserving the physiological membrane environment. In this context, atomic force microscopy (AFM),[35] AFM-based force spectroscopy (AFM-FS)[14, 36] and force clamp (AFM-FC)[37, 38] are essential tools to locally study the physical properties of supported membranes at the nanoscale with high spatial range sensitivity and versatility while giving the possibility to control the environmental conditions. Lateral interactions between the molecules can be directly evaluated with AFM-FS, by measuring the maximum vertical force a membrane is able to resist before its rupture, the breakthrough force F_b, when indented by the AFM tip. This parameter is significantly governed by the chemical structure of the membrane components[39] as well as by the physicochemical environment, especially the presence of ions that can alter the molecular interactions within the membrane.[40-42] Moreover, AFM-FS can differentiate subtle local variations in composition, leading to phase segregation, in terms of both the mechanical stability and membrane thickness associated to the observed topography.[13-15, 26]

Here, we study for the first time the detailed structure of the QS membrane at the nanoscale, using AFM and AFM-FS under controlled liquid environment (ionic medium and temperature) to assess the topography of supported QS membranes (SQMs) and to evaluate the local membrane mechanics. We further perform MD simulations to provide an atomistic interpretation of the obtained results. Our results are direct evidence of the bilayer nature of the QS membrane, with characteristics of a fluid-like membrane, and which structural and mechanical properties depend on the surrounding environment. We demonstrate how ions alter the lateral packing, modifying the membrane mechanics. According to the ionic environment and temperature, we

show that different domains may coexist in the QS membranes, ascribed to variations in molecular tilt angles.

2. RESULTS AND DISCUSSION

2.1. Supported QS membrane structural characterization

For the study at the nanoscale of Chol:CTAB QS bilayer and its mechanical properties, we prepared two different supported QS membranes (SQMs) on mica surfaces using the QS vesicular samples described in Table 1. The samples were prepared following the DELOS-susp procedure,[31] a one-step methodology based on the use of compressed CO_2 which permits the straightforward preparation of the nanoscopic QSs, without further steps of extrusion or thaw-freezing. The mean size of QSs obtained were in the range between 90-150 nm in diameter. The vesicles structural characterization by dynamic light scattering (DLS) and Cryo-TEM are detailed in the SI (Table S1, Figure S1).

Table 1. Composition of vesicles suspensions used to prepare the SQMs.

QS vesicular sample	Membrane components concentration	Aqueous medium
QS_H_2O	7.3 mM CTAB, 7.3 mM	Milli-Q (ultrapure) water

	cholesterol	
QS_PBS	7.3 mM CTAB, 7.3 mM cholesterol	PBS/NaCl pH 7.4 (94 mM NaCl, 4 mM PBS) buffer solution

When exposed to freshly cleaved mica surfaces, QS vesicles open and fuse onto the substrate forming SQMs. This procedure is equivalent to the liposome rupture method[43] based on the formation of a supported lipid bilayer (SLB) by depositing a suspension of liposomes onto a flat surface. This allows for a detailed morphological and nanomechanical characterization at the nanoscale, using atomic force microscopy (AFM) and spectroscopy (AFM-FS), under controlled liquid environment.

2.1.1 Topographical characterization

As shown in Figure 1, QS_H_2O and QS_PBS membranes spread all over the mica surface. At the initiation of the AFM experiment (t_0), after depositing the QSs onto the mica surface for 30 min at room temperature (RT), coexistence of domains of different thickness was identified for SQMs in both liquid environments. The thickness of the different domains was determined from the force-separation curves (Figure S2) performed during the AFM-FS measurements: 4.7 ± 0.2 nm and 4.1 ± 0.3 nm for the higher and lower domains for QS_H_2O membranes, and 5.3 ± 0.4 nm and 4.5 ± 0.4 nm for the higher and lower domains for QS_PBS membranes. SQM in PBS/NaCl are slightly thicker than in water.

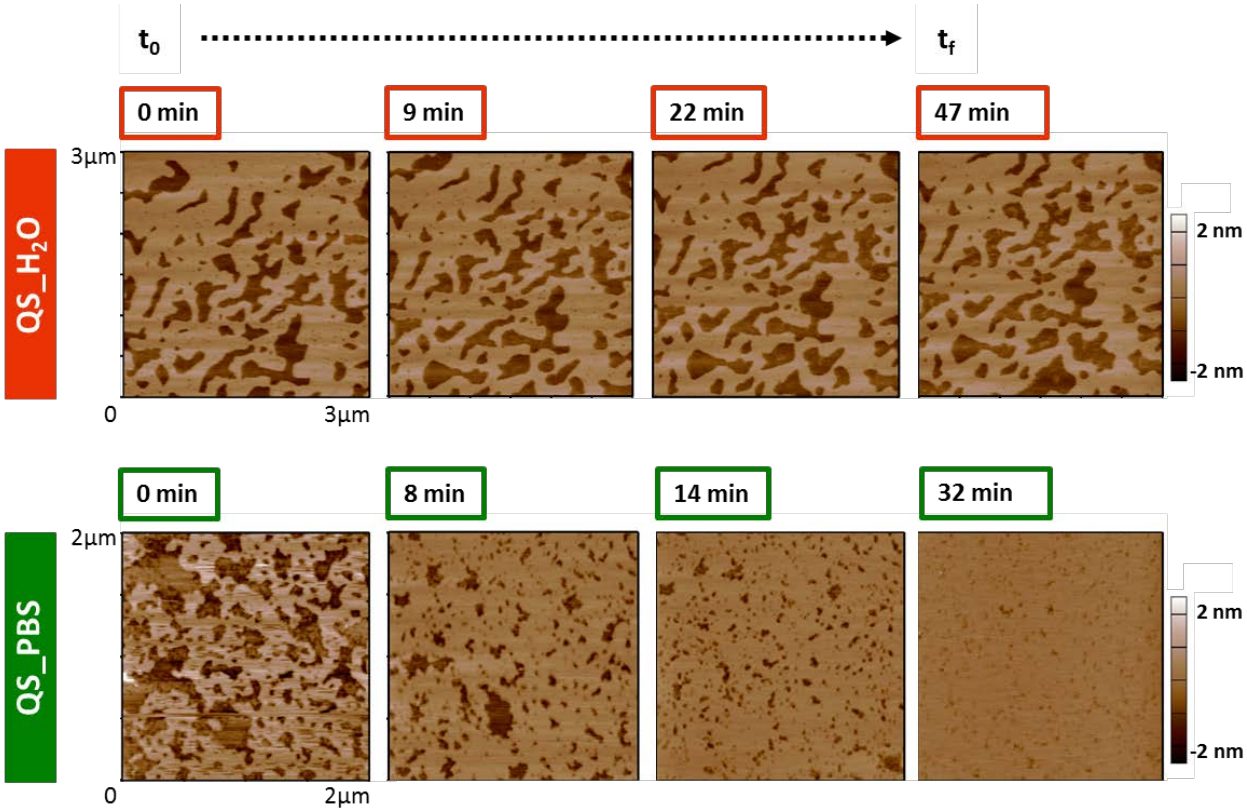

Figure 1. Consecutive AFM AC mode topographical images for SQM on mica in ultrapure water (QS_H_2O) and in PBS/NaCl pH 7.4 (QS_PBS) at RT.

Series of consecutive images over the same area were acquired to study the membrane behavior with time. A steady topography was observed for QS_H_2O (Figure 1, top) after several images (t_f ~ 45 min). Conversely, the QS_PBS membrane showed a dynamic behavior towards a homogeneous bilayer after 30 min (t_f) (Figure 1, bottom). This effect was not a consequence of the imaging as it was verified when imaging different unexplored areas of the same sample after t_f. The membrane at this state had a thickness of 4.9 ± 0.5 nm.

2.1.2 Supported QS membrane nanomechanics

Lateral interactions between the molecules of 2D ordered structures like lipid bilayers can be explored by measuring the maximum force the membrane is able to withstand before its rupture, because of an applied external pressure. In an AFM-FS experiment, the AFM tip breaks through the membrane at a force (the breakthrough force F_b, see Figure S2)[14, 15, 36, 44] that is characteristic of the lateral packing of the membrane of certain composition in a particular environment and at a specific tip velocity.

Force-separation curves were performed over an area of the SQM previously imaged, and we clearly observed the breakthrough events as sharp discontinuities on the approach force-separation curves (Figure S2 and Figure 2c). These sharp breakthroughs at a few nNs are generally characteristic of fluid-like lipid bilayers.[42, 45, 46] We calculated the F_b values at each pixel and built the F_b maps directly correlating the AFM topography. The F_b value of each sample was determined by fitting the F_b distributions to a Gaussian model (Figure 2d). The reported mean F_b for each membrane corresponds to the average of F_b values of 10 samples ± SD (Figure 3).

For QS_H_2O, a bimodal F_b distribution (Figure 2d) is obtained, with mean values of 1.2 ± 0.5 nN and 1.9 ± 0.9 nN. Although the difference is not large, each value is associated to each of the domains, as evidenced in the correlation of the F_b map (Figure 2b) and the topography (Figure 2a), with slightly higher F_b for the thicker domain than for the thinner one. In PBS/NaCl, the initial heterogeneous topography of QS_PBS SQM (Figure 2a, t_0) was also revealed in the F_b map (Figure 2b) with a bimodal F_b distribution, with mean values of 2.5 ± 0.8 nN and 6.3 ± 2.5 nN for the thinner and thicker domains, respectively (Figure 2b-d). Accordingly, at t_f, when the QS_PBS membrane became homogeneous (Figure 2a, t_f), a uniform F_b map (Figure 2b-d) with mean value of 6.2 ± 1.8 nN was obtained, comparable to the value of the thicker domain at t_0.

These F_b values are summarized in Figure 3, and are slightly below the 8.5 ± 2.3 nN of a common lipid membrane: DOPC(1,2-dioleoyl-*sn*-glycero-3-phosphocholine):Chol (80:20) bilayer, prepared from liposomes obtained using the same methodology (Figure S3).

From these data, it becomes clear that the ions in solution play a key role in the lateral packing of the CTA^+ and Chol molecules, leading to an increase in the mechanical resistance of the SQM.

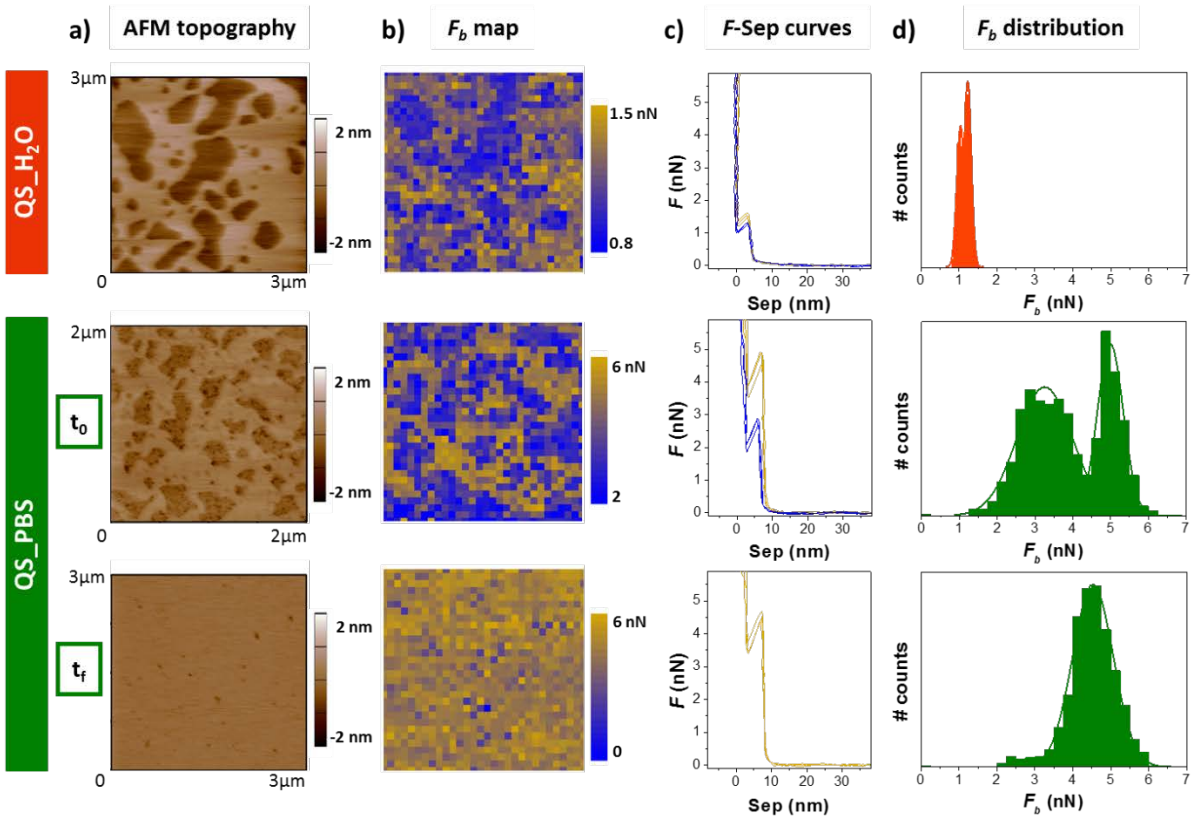

Figura 2. AFM AC-mode topographical images (a) and AFM-FS results (F_b maps (b), force-separation curves (c) and F_b distributions (d)) for representative samples of SQMs on mica in ultrapure water (QS_H_2O) (top) and in PBS/NaCl pH 7.4 (QS_PBS) at t_0 (middle) and t_f (bottom), at RT.

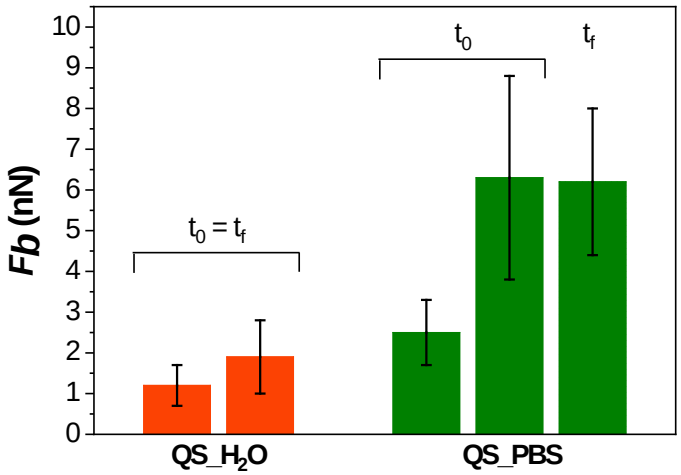

Figure 3. Mean F_b values (± SD) for QS_H_2O (in ultrapure water) and QS_PBS (in PBS/NaCl pH 7.4) SQMs on mica and at RT.

2.2 Role of the ions on the QS membrane topography and nanomechanics

From the topographical and nanomechanical characterization it is evident that the ions present in the liquid environment when the QS assembly takes place are affecting the membrane structure. Not only they may adsorb on the QS surface, but also affect the lateral packing, as the membrane in ionic media shows a higher resistance to break upon indentation. Ions alteration of the nanomechanics of lipid bilayers is a known effect; they have an important contribution to the membrane mechanical resistance, by enhancing the lateral packing, translated into a higher F_b.[41, 42, 46-49]

To better understand the effect of ions into SQMs, we assessed the topographical and mechanical properties of the QS_H_2O membrane before and after replacing the liquid environment from water to PBS/NaCl. Figure 4 shows the topography, F_b maps and histograms for these two cases. From the QS_H_2O membrane with coexisting domains and bimodal F_b distribution, after rinsing

several times with PBS/NaCl, the mechanical stability increases to F_b values close to those of QS_PBS membranes (3.4 ± 0.6 nN for QS_H_2O + PBS, Figure 4). In addition, after PBS/NaCl has been added, the membrane topography and mechanics evolve in time (after *ca*. 50 min) to the one of the SQM from QS_PBS (Figure S4). This means that the ions of the buffer not only affect the membrane properties when QS are produced in PBS/NaCl medium. Ions can also enter and alter the membrane structure upon exposure to the ionic environment, providing a direct evidence that the ions are the direct responsible for the enhancement in lateral interaction and the changes in the membrane mechanics. This atomistic interpretation is confirmed by all-atomic MD simulations in section 2.4.

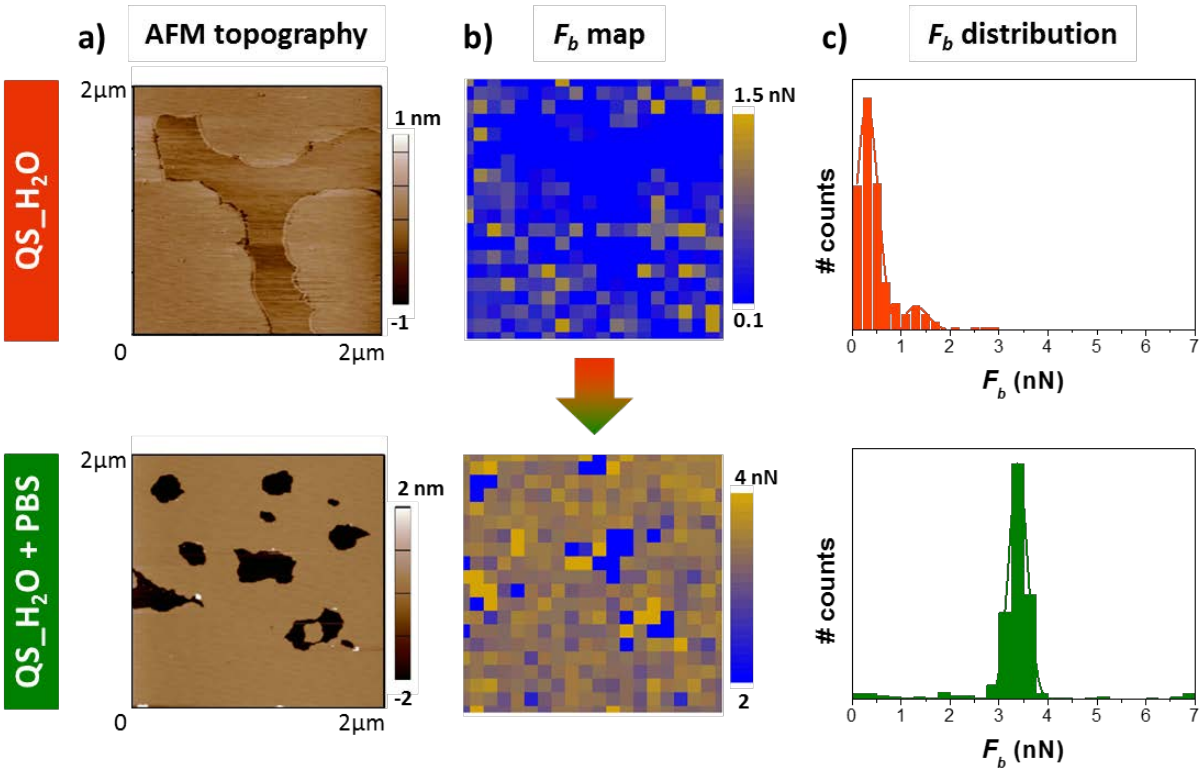

Figure 4. AFM AC mode topographical images (a) and AFM-FS results (F_b maps (b) and distributions (c)) for SQMs on mica in ultrapure water (QS_H_2O) (top) and after the *in situ* addition of PBS/NaCl pH 7.4 (QS_ H_2O + PBS) (bottom) at RT.

2.3 Effect of the temperature on the SQMs structure

From the sharp breakthrough event observed at low F_b values, AFM-FS for the SQMs suggests a typical behavior of a fluid membrane at RT. This type of breakthrough is characteristic of fluid state phospholipid bilayers.[42] In addition, no thermal transition is detected for QS_H_2O or QS_PBS by differential scanning calorimetry for temperatures above RT. This is consistent with previous MD simulations in which the QS components were found to diffuse with similar diffusion coefficient of typical fluid phospholipidic membranes.[33] Still, to understand the origin of the coexisting domains observed in SQMs, we studied the morphology of QS_H_2O and QS_PBS membranes by AFM at different temperatures.

When imaging the SQM in PBS/NaCl, we let the system stabilize to the homogeneous phase at RT, knowing its dynamic behavior at this T. Unsurprisingly, further increase in T up to 45 ºC showed no changes in the QS_PBS membrane topography (Figure S5). Conversely, the QS_H_2O membrane showed a gradual transition from a heterogeneous to a homogeneous topography upon rising T from RT up to 42.5 ºC (Figure 5a and b). Increasing the T stepwise and leaving the membrane at least during 30 min at each temperature, showed that SQMs in water turned into a homogeneous phase around T=30 ºC (Figure 5c and d).

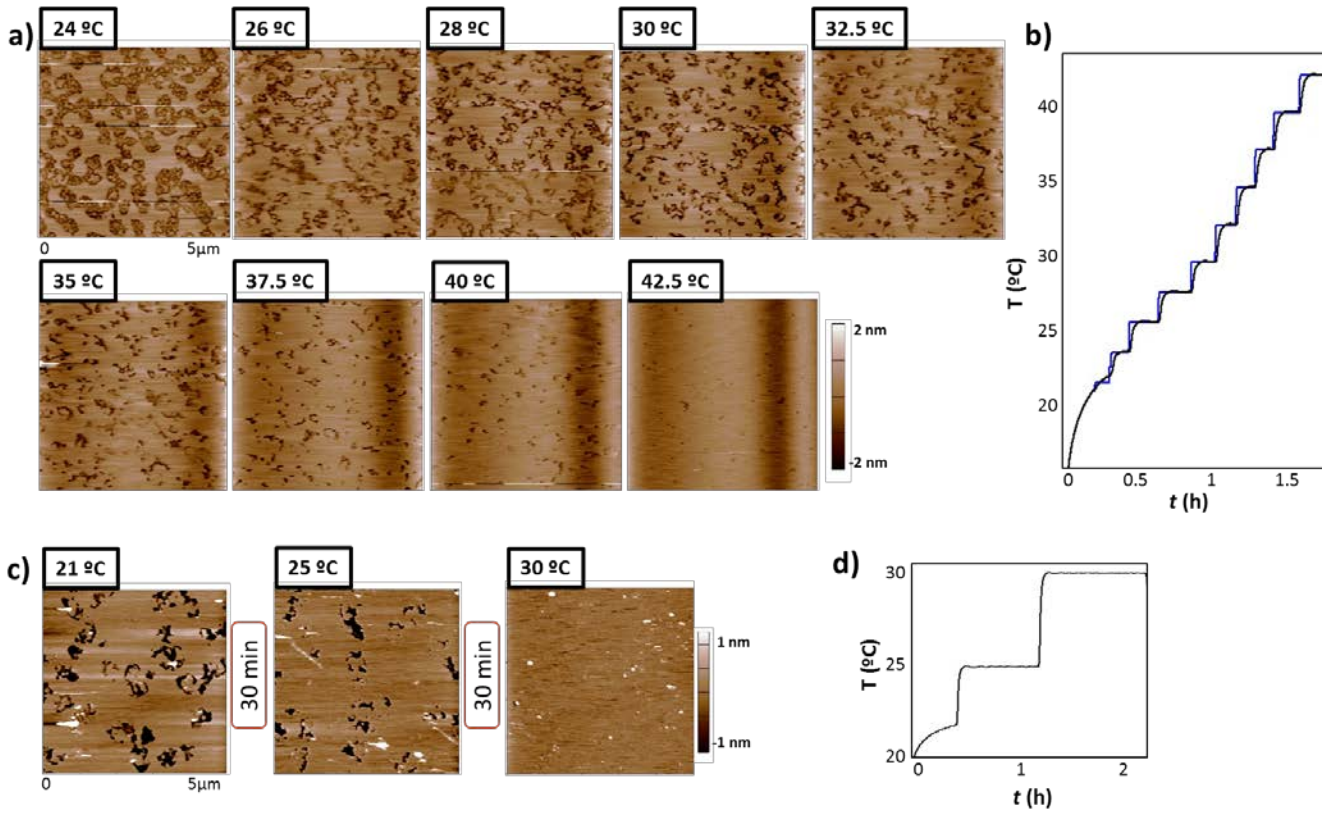

Figure 5. AFM AC-mode topographical images for QS_H_2O membrane supported on mica, in ultrapure water: a) while increasing the experimental temperature following the steps in (b) (blue: set T; black: measured T); c) while increasing the experimental temperature following the steps in (d).

In Figure 6, we propose a molecular interpretation of the heterogeneous topography (phase coexistence) observed for the QS_H_2O membrane. From the AFM measurements, the different domains are associated to different bilayer thickness and very similar, although discernible, nanomechanical resistance. We propose that in the QS_H_2O bilayer the synthon made by CTA^+ and Chol is tilted and that the tilt angle is different in the different regions or domains. Therefore, we propose that the heterogeneities observed are due to different tilt angles, rather than to different chemical compositions.

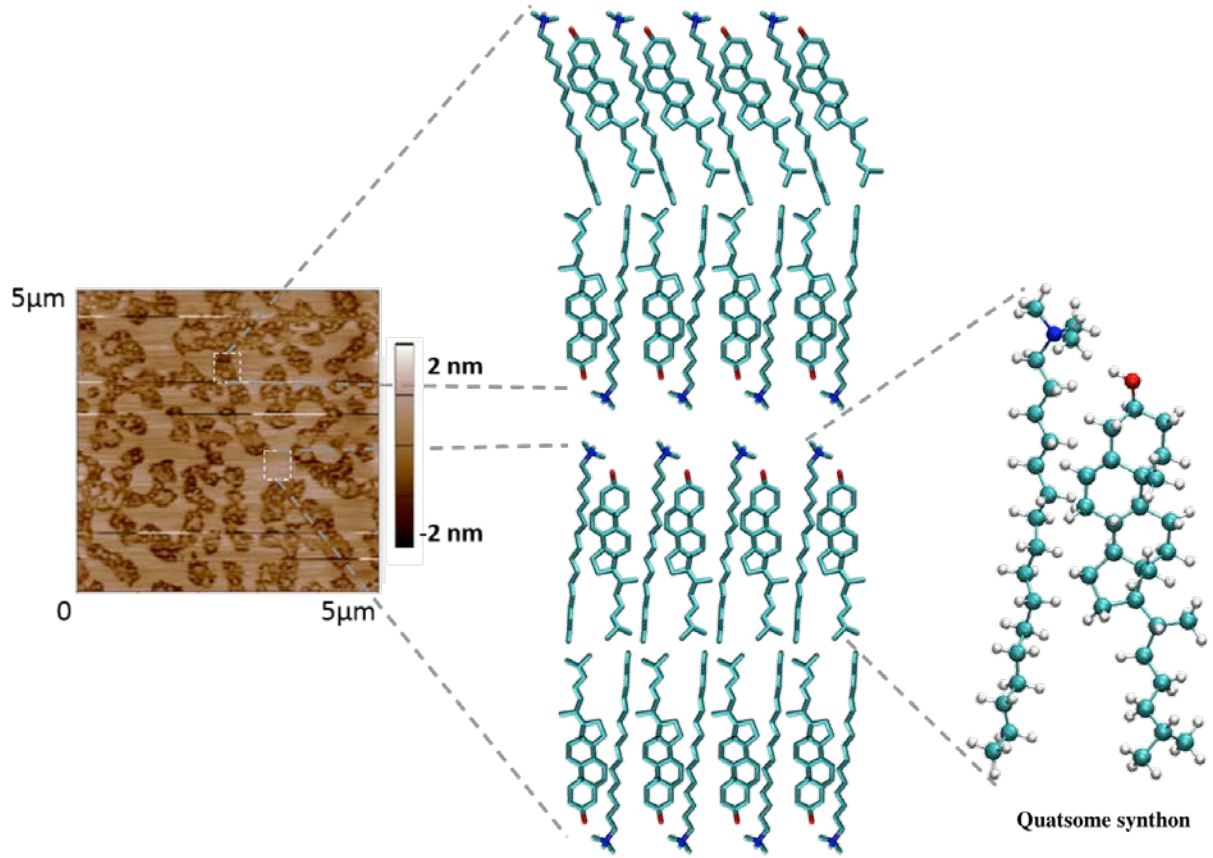

Figure 6. Molecular interpretation of the different topographical domains observed in supported QS_H_2O membranes by AFM, as domains with different tilt for the CTA^+-Chol bimolecular synthon. The CTA^+ and Chol structures are shown in CPK representation.

Regarding this interpretation, it is worth noting that pure CTAB adsorbed onto mica can form bilayers in which the molecules have a substantial tilt of 44° to the surface normal.[50, 51] The bilayer with a well-defined tilt angle is difficult to observe at RT, since this temperature coincides with the Krafft temperature of CTAB (25ºC) and near the Krafft temperature the dynamics of CTA^+ chains is very slow. Previous work shows that the formation of the CTA^+ bilayers at 25ºC has very long equilibration times (6-24 h), and other metastable structures can be observed during equilibration.[52] It has been also proposed that in lipid bilayers with small

Chol concentrations, where all Chol molecules interact independently with the lipid bilayer, Chol has a tilt angle of ~10º and may influence the tilt of the other membrane components.[53] In the QS_H_2O, the bilayer is formed by CTA^+ and Chol that are known to interact strongly forming a 1:1 bimolecular synthon,[29] so it seems possible a complex behaviour for the tilt angle of the components, responsible for the formation of the domains with different tilt proposed in Figure 6. This interpretation is also consistent with the atomistic simulations discussed in the next section.

2.4 Molecular Dynamics (MD) Simulations

We performed all-atomic MD simulations to provide an atomistic interpretation of the experimental results, regarding both the possible penetration of the ions and the possible changes in tilt of the bilayer components. To this end, we have extended to larger simulation times our previous all-atomic MD simulations of QS_H_2O bilayer at 25ºC.[29] In these simulations, we considered a small bilayer patch (~15.7 nm^2) with a 1:1 mixture of CTAB surfactant and Chol in water (there is no supporting surface in the simulations). All technical details of the simulation are the same as in our previous work,[29] with the only difference that the simulation was extended for an additional time of 106 ns. In addition, we have also performed a second simulation in order to evaluate the effect of added salt. In this second simulation, we have added 100 mM of NaCl to our previous simulation of the QS_H_2O bilayer at 25ºC (see methods for details).

The simulations of the QS_H_2O system show that Br^- counterions are not only able to adsorb on top of the bilayer but also to penetrate in the hydrophilic region of the bilayer. In the case of the simulations with added salt (100 mM of NaCl) we also observe that both anions (Br^- counterions

and the Cl^- anions from added salt) penetrate in the hydrophilic region of the bilayer. The results for the organization of the anions in both simulations are summarized in Figure 7.

As seen in Figure 7a, the anions that penetrate inside the bilayer are shared between the CTA^+ headgroup and the –OH group from the Chol. In other words, anions not only interact strongly with cationic CTA^+ surfactant but also with Chol. It is also worth noting that previous experimental and simulation work on pure Chol monolayers has shown a strong interaction between Cl^- and Chol.[49] Here the simulations indicate that the addition of NaCl produces not only an incorporation of Cl^- inside the bilayer but also an incorporation of Br^- inside the bilayer. In the simulations of the QS_H_2O system (being the Br^- counterions the only ions present), we observe that 10% of CTA^+ molecules have a Br^- ion adsorbed on top and a 72% of the CTA^+ molecules have a Br^- ion shared with cholesterol (Figure 7b). In the simulations with added NaCl, we observe that 8% of CTA^+ molecules have a Br^- adsorbed on top and 2% of CTA^+ molecules have Cl^- anions adsorbed on top, while a 66% Br^- and 9% have Cl^- ions are shared with Chol (hence a total of 75% of CTA^+-Chol synthons share an anion). These simulations results are thus compatible with the experimentally observed increase in the F_b after the addition of ions (Figures 2, 3 and 4), which is interpreted as due to the penetration of ions into the hydrophilic region of the QS bilayer (the one occupied by the headgroups) and affect the bilayer structure, as generally seen in phospholipid bilayers.[42, 46, 47, 54, 55]

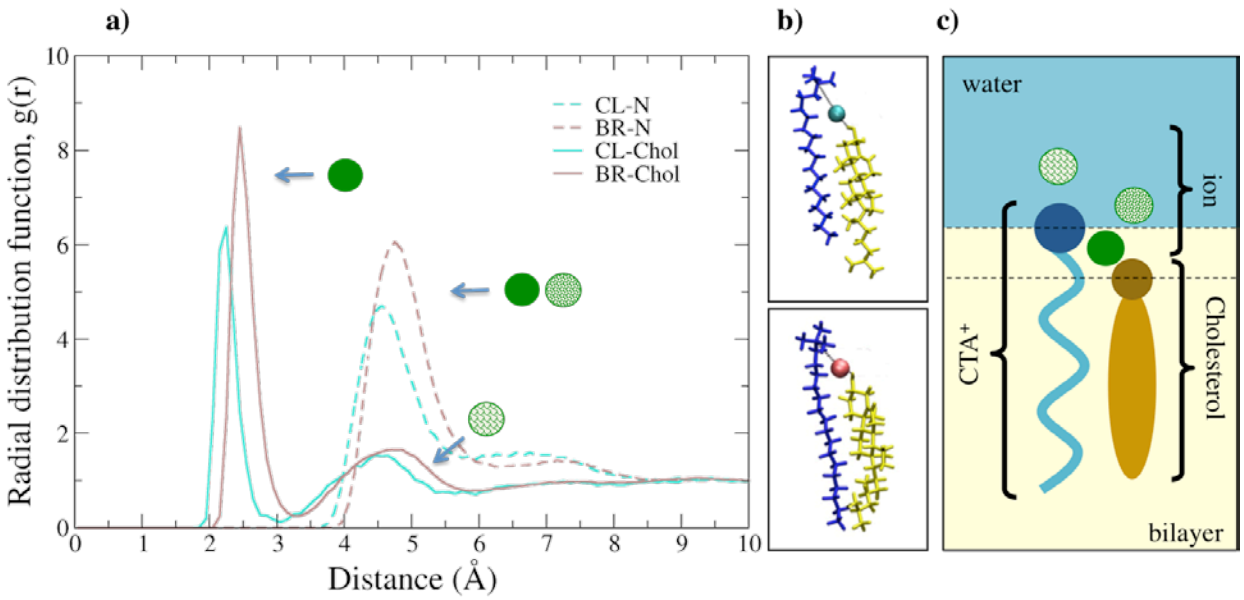

Figure 7. Interaction of anions with the QS components according to MD simulations at 25ºC. a) Radial correlation function g(r) computed between the anions (Br^- or Cl^-) and the polar headgroups (O atom of Chol or N atom of CTA^+) calculated from simulations. b) Snapshots of molecular configurations extracted from MD simulations that contribute to the g(r) function shown in (a). CTA^+ molecule is shown in blue, Chol molecule in yellow and ions as Van der Waals spheres (Cl^- cyan, Br^- brown). c) Cartoon showing schematically the ionic correlations found in the simulations. A full sphere indicates that the peak corresponds to adsorption of an anion inside the bilayer, shared between CTA^+ and Chol and a dotted sphere indicates that the peak corresponds to an anion adsorbed on top of a CTA^+ molecule, as indicated in (a).

We have also analyzed the tilt angle of both CTA^+ and Chol molecules in the bilayers. The results for the QS_H_2O bilayer are shown in Figure 8 and the results for the simulation with added NaCl are shown in the SI, Figure S6. We show the results for the tilt angle of CTA^+ and representative snapshots of the bilayer, showing the tilt of both CTA^+ and Chol molecules. For Chol the tilt was always the same than the one reported for CTA^+ (data not shown), so the tilt

angles in Figure 8 correspond to the tilt of the CTA^+-Chol synthon. The first remarkable observation is that the symmetry within the bilayer is spontaneously broken, in the sense that the CTA^+ surfactant molecules have different tilt in each leaflet of the bilayer. It is interesting to note that an analogous symmetry breaking has been previously observed in MD simulations of other stable vesicles (catanionic surfactant vesicles).[56]

More importantly, not only the average tilt angle is different in each leaflet of the bilayer but also the behavior of the tilt angle as a function of time is different. In one of the leaflets, the CTA^+ fluctuates around an average tilt of 10º (Figure 8). In the other leaflet, the CTA^+ molecules jump between states with different tilt (~13º and 15º), remaining in these states during times of 20-30 ns, which are substantial at the scale of the simulated system. In the case of simulations with added NaCl (Figure S6 and S7), we observe again that CTA^+ molecules from the two leaflets have different average tilt angles (10º and 14º respectively) but the ~20 ns jumps observed in absence of salt are not observed in presence of added salt. In this case, the fluctuation between different orientations take place at much shorter time scales, of the order of the ns or less (Figure S6).

Formation of heterogeneities (domains coexistence) is not observable by MD simulations due to the small size of the simulated systems (15.7 nm^2). Besides, it is also important to consider that the underlying substrate on the AFM experiments may affect the lateral packing of the bilayer.[15, 57-60] Still, the existence of different orientations for the CTA^+ (and Chol) molecule in the small simulated QS_H_2O systems suggest the possibility of the existence of different nanoscale domains with different tilt angle for the molecules in the QS_H_2O SQMs as proposed in Figure 6 from AFM results. It is also interesting to note that according to the experimental results (Figure

2) the addition of salt suppresses the presence of heterogeneous domains. This is also consistent with the simulation results shown in Figure S6 (absence of long-lived different states with different tilt angle).

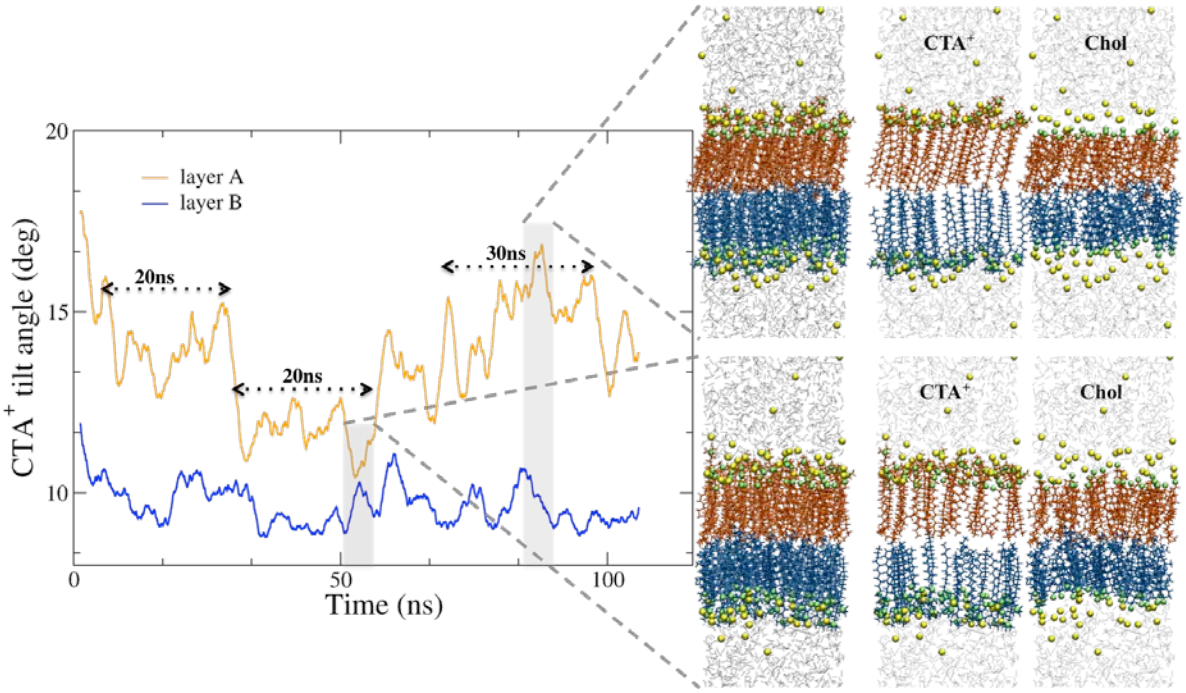

Figure 8. Results obtained in MD simulations of a QS_H_2O bilayer at 25 ºC (no added salt). The left plot shows the tilt angle for CTA^+ molecules (averaged over a leaflet) *vs*. time during the MD simulations. The data for each leaflet of the bilayer is indicated in a different color. The residence time into different states with different tilt angles are indicated in the figure. Right: representative snapshots of the states indicated in grey in the left plot. For each case we show the full bilayer and to facilitate the visualization we also show partial views with only CTA^+ or only Chol molecules. The molecules at each leaflet are colored different (blue or orange) in correspondence with the left plot. N atoms from the CTA^+ headgroups are indicated as green spheres and Br^- ions are shown as yellow spheres. The shadow region corresponds to the region occupied by water molecules.

3. CONCLUSIONS

We characterized for the first time the topography and the nanomechanical properties of supported QS membranes in different liquid environment and T. We determined experimentally that the QS membrane behaves as a typical fluid-like phospholipid bilayer. A phase-segregated topography, stable with time, was observed by AFM in supported QS_H_2O membranes, while in the presence of salts supported QS_PBS membranes showed a dynamic behavior from a heterogeneous topography turning into a homogeneous phase at RT.

By means of AFM-FS, we showed that the membrane breaks upon indentation with the AFM tip, as observed for 2D ordered systems like lipid bilayers and we further determined the effect of the presence of ions into the liquid media over the nanomechanical resistance of the QS membrane. We observed by MD simulations that the anions from solution (both Br^- and Cl^-) not only adsorb onto the bilayer but also penetrate the hydrophilic region of the bilayer. As a result, an enhancement of the lateral interactions between the membrane molecules may be the responsible of the greater resistance to be indented by the AFM tip (higher F_b) in the presence of salts.

We demonstrate that the phase coexistence observed at RT in the QS_H_2O SQM turns into a homogeneous structure when temperature is raised above 30ºC. All-atomic MD simulations of QS bilayer at 25ºC in absence of added salts showed that the symmetry within the bilayer is spontaneously broken, with different molecular tilt in each leaflet, one of the leaflets jumping within two possible orientations within 20-30 ns. The coexistence of different nanoscale domains may therefore be associated to different tilt angle for the molecules in the QS_H_2O SQMs measured with AFM.

The nanomechanical behavior observed indicate that QS are formed by a bilayer membrane with a compact structure homogeneous in composition, and with comparable properties to fluid-like lipid bilayers, but with the benefit of a great colloidal stability. The variations observed with the incorporation of salts suggest that the membrane properties may be easily tuned by altering the lateral interactions, either with different environmental ions or counterions, or even by choosing a specific surfactant headgroup. These results place QS as very promising candidates for deformable and flexible nanovesicles alternatives, highly pursued in nanomedicine applications exploring the transdermal administration route.[61]

4. METHODS

4.1 Materials

Cholesterol (Chol) 5-Cholesten-3*β*-ol from Panreac (Spain) and cetyltrimethylammonium bromide (CTAB) from Aldrich, were used without further purification. The experiments were performed in ultrapure water (Milli-Q reverse osmosis system, 18.2 mΩ·cm resistivity) or in PBS/NaCl buffer solution pH 7.4 (94 mM NaCl, 4 mM phosphate buffer saline (PBS)). For the AFM experiments the buffer solution was filtered through a 0.22 μm pore size inorganic membrane before use.

4.2 Cholesterol:CTAB Quatsomes (QS) preparation

Cholesterol:CTAB (1:1 molar ratio) QS were made by DELOS-SUSP (depressurization of an expanded liquid organic solution-suspension) method as described in refs (Cabrera, I.; Elizondo, E.; Esteban, O.; Corchero, J. L.; Melgarejo, M.; Pulido, D.; Córdoba, A.; Moreno, E.; Unzueta, U.; Vazquez, E.; Abasolo, I.; Schwartz, S.; Villaverde, A.; Albericio, F.; Royo, M.; Garcia-

Parajo, M. F.; Ventosa, N.; Veciana, J. Multifunc- tional Nanovesicle-Bioactive Conjugates Prepared by a One-Step Scalable Method Using CO2-Expanded Solvents. Nano Lett. 2013, 13, 3766−3774) and (Grimaldi, N.; Andrade, F.; Segovia, N.; Ferrer-Tasies, L.; Sala, S.; Veciana, J.; Ventosa, N. Lipid-based Nanovesicles for Nano- medicine. Chem. Soc. Rev. 2016, 45, 6520−6545.) Briefly, a 7.5 mL high-pressure vessel was loaded with a solution of 76 mg of Chol in 2.88 mL of ethanol at atmospheric pressure and 35 °C. Then, the reactor vessel was pressurized with compressed CO_2, producing a volumetric expanded liquid solution, at a pressure of 10 MPa, a CO_2 molar fraction of $X_{CO2} = 0.62$ and a temperature of 35 °C. The system was kept at 35 °C and 10 MPa for 1 h. Finally, the CO_2-expanded Chol solution was removed from the reactor through a depressurization valve and collected in 24 mL of aqueous solution, either ultrapure water or PBS/NaCl pH 7.4 (94 mM NaCl, 4 mM PBS) buffer depending on the formulation, with 72 mg of dissolved CTAB. In this final step, where the Chol:CTAB quatsomes are formed, a flow of N_2 is used as a plunger to push down the CO_2-expanded solution from the vessel and to maintain a constant pressure inside the vessel during depressurization. The molar ratio between the CTAB and the Chol in the final formulation was 1 to 1, which has been shown to be the correct proportion in order to have a pure vesicular phase (Ferrer-Tasies, L.; Moreno-Calvo, E.; Cano-Sarabia, M.; Aguilella-Arzo, M.; Angelova, A.; Lesieur, S.; Ricart, S.; Faraudo, J.; Ventosa, N.; Veciana, J. Quatsomes: Vesicles Formed by Self-Assembly of Sterols and Quaternary Ammonium Surfactants. Langmuir 2013, 29, 6519−6528).

.

4.3 Supported membranes

SQMs were obtained by direct fusion onto freshly cleaved mica surfaces (mica discs, Ted Pella, Redding, CA) previously glued onto Teflon discs using epoxy-based mounting glue. 100 µL of QS suspension (2.75 mg ml^{-1}) were deposited on to the mica for 30 min at RT. Afterwards, the samples were rinsed several times with water or PBS/NaCl buffer to remove unfused vesicles, keeping always the samples hydrated.

4.4 Atomic force microscopy (AFM) and spectroscopy (AFM-FS)

AFM images and force spectroscopy experiments were performed using an MFP-3D atomic force microscope (Asylum Research) using V-shaped Si_3N_4 cantilevers with Si_3N_4 tips and nominal spring constants of 0.35 N m^{-1} or 0.24 N m^{-1} (DNP, Bruker AFM Probes). The cantilever spring constants were individually calibrated using the equipartition theorem (thermal noise routine)[62] in air conditions, after measuring the sensitivity (V m^{-1}) on a silicon substrate. The same equipartition theorem was afterwards employed again to calculate the sensitivity on the required liquid environment. When required, temperature control was achieved with a T-controlled sample stage (BioHeater, Asylum Research).

AFM images over areas from 0.5 x 0.5 to 5 x 5 μm^2 were acquired in AC mode at RT and under liquid conditions (Milli-Q water or PBS/NaCl buffer solution). After imaging the selected region, AFM-FS was performed by approaching and retracting the AFM tip to the sample at a constant velocity of 1 µm s^{-1}. The force-separation curves were recorded by following an array of points from 20 x 20 to 30 x 30 (force map mode) over an imaged area. A home-made Python program based on ref.[63] was used to analyze the force-separation curves from the grids and evaluate the breakthrough force (F_b) values. Mean F_b values are obtained from the gaussian fits and expressed ± SD. The membrane thickness was calculated from the force-separation curves,

taking the distance between the tip-membrane initial contact and the point at which tip and mica are in contact (Figure S2).

4.5 Molecular dynamics (MD)

MD simulations consist of solving numerically the Newton equations of motion for a molecular system. In our simulations, we describe all chemical species (water, Chol, CTAB and ions) with full atomistic detail. The simulated system QS_H_2O consists of two leaflets of 27 CTA^+ and 27 Chol molecules (equilibrium area ~15.7 nm^2) each and 54 Br^- ions immersed in 5443 TIP3P water molecules. The simulations were performed using the NPTγ ensemble maintaining the QS bilayer at 25ºC, 1 atm of pressure and zero tension to mimic a vesicle bilayer. The employed force field and all technical details of the simulation are the same as in our previous work,[29] with the only difference that the simulation was extended for an additional time of 106 ns using the NAMD 2.11 software.[64] An additional simulation with added salt was performed starting from the previous simulation QS_H_2O (with no added salt). Starting from an equilibrated configuration of the QS_H_2O, we added 10 Na^+ and 10 Cl^- ions (roughly corresponding to ~100 mM) using the ionize plugin of the VMD program. After equilibration and thermalization, we ran a simulation of 131 ns employing the same parameters and conditions as in the QS_H_2O case. The analysis of both simulations (snapshots, radial correlation functions, …) was performed using VMD software.[65]

ASSOCIATED CONTENT

Supporting Information. QS vesicle structural characterization. Schematic figure on AFM-FS on lipid membranes. Mechanical properties of DOPC:Chol (80:20) membrane. Additional results on AFM characterization of SQMs from QS_H_2O after changing to PBS/NaCl and SQMs from

QS_PBS with T. Additional results on MD simulations of a QS bilayer with added salt (NaCl) and tilt angles of CTA^+ with water and with added salt. This material is available free of charge via the Internet at http://pubs.acs.org.

AUTHOR INFORMATION

Corresponding Author

*E-mail: jfaraudo@icmab.es (Simulations)

*E-mail: ventosa@icmab.es

*E-mail: migiannotti@ibecbarcelona.eu

Present Addresses

¶Laboratory of Self-Organizing Soft Matter and Laboratory of Macromolecular and Organic Chemistry, Department of Chemical Engineering and Chemistry; Institute for Complex Molecular Systems, Eindhoven University of Technology, Eindhoven (The Netherlands).

†Physics and Astronomy department, University of Sheffield, Sheffield (UK).

Author Contributions

The manuscript was written through contributions of all authors. All authors have given approval to the final version of the manuscript.

Funding Sources

Generalitat de Catalunya (AGAUR, 2017 SGR 918 and 2017 SGR 1442), the Spanish Ministry of Economy and Competitiveness (MINECO), through the ‘‘Severo Ochoa’’ Programme for Centres of Excellence in R&D (Grant SEV-2015-0496), the MINECO and FEDER (CTQ2015-66194-R and MAT2016-80826-R projects), the Instituto de Salud Carlos III, through “Acciones CIBER” and CIBER-BBN FlexQS-skin project, and the COST Action CA15126.

ACKNOWLEDGMENT

We acknowledge financial support from the Generalitat de Catalunya (AGAUR, 2017 SGR 918 and 2017 SGR 1442), the Spanish Ministry of Economy and Competitiveness (MINECO), through the ‘‘Severo Ochoa’’ Programme for Centres of Excellence in R&D with Grant SEV-2015-0496, the MINECO and FEDER for the CTQ2015-66194-R and MAT2016-80826-R projects, the Instituto de Salud Carlos III, through “Acciones CIBER” and CIBER-BBN FlexQS-skin project, and the COST Action CA15126. We thank CESGA Supercomputing Center for technical support and the use of computational resources. The computer simulations reported in this work have been developed under the Material Science PhD program in the Barcelona Autonomous University (UAB).

REFERENCES

1. Allen, T. M.; Cullis, P. R., Drug Delivery Systems: Entering the Mainstream. *Science* **2004,** *303* (5665), 1818.
2. Duncan, R.; Gaspar, R., Nanomedicine(s) under the Microscope. *Molecular Pharmaceutics* **2011,** *8* (6), 2101-2141.
3. Ahmad, M. Z.; Akhter, S.; Jain, G. K.; Rahman, M.; Pathan, S. A.; Ahmad, F. J.; Khar, R. K., Metallic nanoparticles: technology overview & drug delivery applications in oncology. *Expert Opinion on Drug Delivery* **2010,** *7* (8), 927-942.

4. Duncan, R.; Vicent, M. J., Polymer therapeutics-prospects for 21st century: The end of the beginning. *Advanced Drug Delivery Reviews* **2013,** *65* (1), 60-70.
5. Torchilin, V. P., Recent advances with liposomes as pharmaceutical carriers. *Nature Reviews Drug Discovery* **2005,** *4*, 145.
6. Goldberg, M.; Langer, R.; Jia, X., Nanostructured materials for applications in drug delivery and tissue engineering. *Journal of biomaterials science. Polymer edition* **2007,** *18* (3), 241-268.
7. Sawant, R. R.; Torchilin, V. P., Liposomes as 'smart' pharmaceutical nanocarriers. *Soft Matter* **2010,** *6* (17), 4026-4044.
8. Grimaldi, N.; Andrade, F.; Segovia, N.; Ferrer-Tasies, L.; Sala, S.; Veciana, J.; Ventosa, N., Lipid-based nanovesicles for nanomedicine. *Chemical Society Reviews* **2016,** *45* (23), 6520-6545.
9. Canton, I.; Battaglia, G., Endocytosis at the nanoscale. *Chemical Society Reviews* **2012,** *41* (7), 2718-2739.
10. Zeb, A.; Qureshi, O. S.; Kim, H.-S.; Cha, J.-H.; Kim, H.-S.; Kim, J.-K., Improved skin permeation of methotrexate via nanosized ultradeformable liposomes. *International Journal of Nanomedicine* **2016,** *11*, 3813-3824.
11. Dimova, R., Recent developments in the field of bending rigidity measurements on membranes. *Advances in Colloid and Interface Science* **2014,** *208*, 225-234.
12. Vorselen, D.; MacKintosh, F. C.; Roos, W. H.; Wuite, G. J. L., Competition between Bending and Internal Pressure Governs the Mechanics of Fluid Nanovesicles. *ACS Nano* **2017,** *11* (3), 2628-2636.
13. Gumi-Audenis, B.; Sanz, F.; Giannotti, M. I., Impact of galactosylceramides on the nanomechanical properties of lipid bilayer models: an AFM-force spectroscopy study. *Soft Matter* **2015,** *11* (27), 5447-5454.
14. Gumí-Audenis, B.; Costa, L.; Carlà, F.; Comin, F.; Sanz, F.; Giannotti, I. M., Structure and Nanomechanics of Model Membranes by Atomic Force Microscopy and Spectroscopy: Insights into the Role of Cholesterol and Sphingolipids. *Membranes* **2016,** *6* (4), 58.
15. Redondo-Morata, L.; Giannotti, M. I.; Sanz, F., Influence of cholesterol on the phase transition of lipid bilayers: a temperature-controlled force spectroscopy study. *Langmuir* **2012,** *28* (35), 12851-60.
16. Bloom, M.; Evans, E.; Mouritsen, O. G., Physical properties of the fluid lipid-bilayer component of cell membranes: a perspective. *Quarterly Reviews of Biophysics* **1991,** *24* (3), 293-397.
17. Needham, D.; Nunn, R. S., Elastic deformation and failure of lipid bilayer membranes containing cholesterol. *Biophysical Journal* **1990,** *58* (4), 997-1009.
18. Briuglia, M.-L.; Rotella, C.; McFarlane, A.; Lamprou, D. A., Influence of cholesterol on liposome stability and on in vitro drug release. *Drug Delivery and Translational Research* **2015,** *5* (3), 231-242.
19. Hosta-Rigau, L.; Zhang, Y.; Teo, B. M.; Postma, A.; Stadler, B., Cholesterol - a biological compound as a building block in bionanotechnology. *Nanoscale* **2013,** *5* (1), 89-109.
20. Bozzuto, G.; Molinari, A., Liposomes as nanomedical devices. *International Journal of Nanomedicine* **2015,** *10*, 975-999.
21. Vorselen, D.; Marchetti, M.; Lopez-Iglesias, C.; Peters, P. J.; Roos, W. H.; Wuite, G. J. L., Multilamellar nanovesicles show distinct mechanical properties depending on their degree of lamellarity. *Nanoscale* **2018,** *10* (11), 5318-5324.

22. Romero, E.; Jose Morilla, M., *Ultradeformable phospholipid vesicles as a drug delivery system: a review*. 2015; p 55.
23. Hussain, A.; Singh, S.; Sharma, D.; Webster, T. J.; Shafaat, K.; Faruk, A., Elastic liposomes as novel carriers: recent advances in drug delivery. *International Journal of Nanomedicine* **2017,** *12*, 5087-5108.
24. Franzé, S.; Donadoni, G.; Podestà, A.; Procacci, P.; Orioli, M.; Carini, M.; Minghetti, P.; Cilurzo, F., Tuning the Extent and Depth of Penetration of Flexible Liposomes in Human Skin. *Molecular Pharmaceutics* **2017,** *14* (6), 1998-2009.
25. Elsayed, M. M. A.; Ibrahim, M. M.; Cevc, G., The effect of membrane softeners on rigidity of lipid vesicle bilayers: Derivation from vesicle size changes. *Chemistry and Physics of Lipids* **2018,** *210*, 98-108.
26. Lima, L. M.; Giannotti, M. I.; Redondo-Morata, L.; Vale, M. L.; Marques, E. F.; Sanz, F., Morphological and nanomechanical behavior of supported lipid bilayers on addition of cationic surfactants. *Langmuir* **2013,** *29* (30), 9352-61.
27. Akbarzadeh, A.; Rezaei-Sadabady, R.; Davaran, S.; Joo, S. W.; Zarghami, N.; Hanifehpour, Y.; Samiei, M.; Kouhi, M.; Nejati-Koshki, K., Liposome: classification, preparation, and applications. *Nanoscale Research Letters* **2013,** *8* (1), 102.
28. Cano-Sarabia, M.; Angelova, A.; Ventosa, N.; Lesieur, S.; Veciana, J., Cholesterol induced CTAB micelle-to-vesicle phase transitions. *Journal of Colloid and Interface Science* **2010,** *350* (1), 10-15.
29. Ferrer-Tasies, L.; Moreno-Calvo, E.; Cano-Sarabia, M.; Aguilella-Arzo, M.; Angelova, A.; Lesieur, S.; Ricart, S.; Faraudo, J.; Ventosa, N.; Veciana, J., Quatsomes: Vesicles Formed by Self-Assembly of Sterols and Quaternary Ammonium Surfactants. *Langmuir* **2013,** *29* (22), 6519-6528.
30. Elizondo, E.; Larsen, J.; Hatzakis, N. S.; Cabrera, I.; Bjørnholm, T.; Veciana, J.; Stamou, D.; Ventosa, N., Influence of the Preparation Route on the Supramolecular Organization of Lipids in a Vesicular System. *Journal of the American Chemical Society* **2012,** *134* (4), 1918-1921.
31. Cabrera, I.; Elizondo, E.; Esteban, O.; Corchero, J. L.; Melgarejo, M.; Pulido, D.; Córdoba, A.; Moreno, E.; Unzueta, U.; Vazquez, E.; Abasolo, I.; Schwartz, S.; Villaverde, A.; Albericio, F.; Royo, M.; García-Parajo, M. F.; Ventosa, N.; Veciana, J., Multifunctional Nanovesicle-Bioactive Conjugates Prepared by a One-Step Scalable Method Using CO2-Expanded Solvents. *Nano Letters* **2013,** *13* (8), 3766-3774.
32. Liu, X.; Ardizzone, A.; Sui, B.; Anzola, M.; Ventosa, N.; Liu, T.; Veciana, J.; Belfield, K. D., Fluorenyl-Loaded Quatsome Nanostructured Fluorescent Probes. *ACS Omega* **2017,** *2* (8), 4112-4122.
33. Ardizzone, A.; Kurhuzenkau, S.; Illa-Tuset, S.; Faraudo, J.; Bondar, M.; Hagan, D.; Van Stryland Eric, W.; Painelli, A.; Sissa, C.; Feiner, N.; Albertazzi, L.; Veciana, J.; Ventosa, N., Nanostructuring Lipophilic Dyes in Water Using Stable Vesicles, Quatsomes, as Scaffolds and Their Use as Probes for Bioimaging. *Small* **2018,** *14* (16), 1703851.
34. Santana, H.; Ventosa, N.; Martinez, E.; Berlanga, J. A.; Cabrera, I.; Veciana, J. Vesicles which include epidermal growth factor and compositions that contain same. WO2014/019555.
35. Dufrêne, Y. F.; Ando, T.; Garcia, R.; Alsteens, D.; Martinez-Martin, D.; Engel, A.; Gerber, C.; Müller, D. J., Imaging modes of atomic force microscopy for application in molecular and cell biology. *Nature Nanotechnology* **2017,** *12*, 295.

36. Redondo-Morata, L.; Giannotti, M. I.; Sanz, F., Stability of Lipid Bilayers as Model Membranes: Atomic Force Microscopy and Spectroscopy Approach. In *Atomic force microscopy in Liquid: Biological Applications*, First Edition ed.; Baró, A. M.; Reifenberger, R. G., Eds. Wiley-VCH Verlag & Co. KGaA: Weinheim, Germany, 2012; pp 259-284.
37. Redondo-Morata, L.; Giannotti, M. I.; Sanz, F., AFM-based force-clamp monitors lipid bilayer failure kinetics. *Langmuir* **2012,** *28* (15), 6403-10.
38. Relat-Goberna, J.; Beedle Amy, E. M.; Garcia-Manyes, S., The Nanomechanics of Lipid Multibilayer Stacks Exhibits Complex Dynamics. *Small* **2017,** *13* (24), 1700147.
39. Garcia-Manyes, S.; Redondo-Morata, L.; Oncins, G.; Sanz, F., Nanomechanics of Lipid Bilayers: Heads or Tails? *Journal of the American Chemical Society* **2010,** *132* (37), 12874-12886.
40. Garcia-Manyes, S.; Oncins, G.; Sanz, F., Effect of temperature on the nanomechanics of lipid bilayers studied by force spectroscopy. *Biophysical Journal* **2005,** *89* (6), 4261-4274.
41. Garcia-Manyes, S.; Oncins, G.; Sanz, F., Effect of pH and ionic strength on phospholipid nanomechanics and on deposition process onto hydrophilic surfaces measured by AFM. *Electrochimica Acta* **2006,** *51* (24), 5029-5036.
42. Redondo-Morata, L.; Giannotti, M. I.; Sanz, F., Structural impact of cations on lipid bilayer models: Nanomechanical properties by AFM-force spectroscopy. *Molecular Membrane Biology* **2014,** *31* (1), 17-28.
43. Mingeot-Leclercq, M. P.; Deleu, M.; Brasseur, R.; Dufrene, Y. F., Atomic force microscopy of supported lipid bilayers. *Nature Protocols* **2008,** *3* (10), 1654-1659.
44. Dufrêne, Y. F.; Lee, G. U., Advances in the characterization of supported lipid films with the atomic force microscope. *Biochimica et Biophysica Acta (BBA) - Biomembranes* **2000,** *1509* (1), 14-41.
45. Garcia-Manyes, S.; Sanz, F., Nanomechanics of lipid bilayers by force spectroscopy with AFM: A perspective. *Biochimica Et Biophysica Acta-Biomembranes* **2010,** *1798* (4), 741-749.
46. Redondo-Morata, L.; Oncins, G.; Sanz, F., Force Spectroscopy Reveals the Effect of Different Ions in the Nanomechanical Behavior of Phospholipid Model Membranes: The Case of Potassium Cation. *Biophysical Journal* **2012,** *102* (1), 66-74.
47. Garcia-Manyes, S.; Oncins, G.; Sanz, F., Effect of ion-binding and chemical phospholipid structure on the nanomechanics of lipid bilayers studied by force spectroscopy. *Biophysical Journal* **2005,** *89*, 1812-1826.
48. Faraudo, J.; Travesset, A., Phosphatidic Acid Domains in Membranes: Effect of Divalent Counterions. *Biophysical Journal* **2007,** *92* (8), 2806-2818.
49. Del Castillo-Santaella, T.; Maldonado-Valderrama, J.; Faraudo, J.; Martín-Molina, A., Specific Ion Effects in Cholesterol Monolayers. *Materials* **2016,** *9* (5), 340.
50. Griffin, L. R.; Browning, K. L.; Truscott, C. L.; Clifton, L. A.; Clarke, S. M., Complete Bilayer Adsorption of C16TAB on the Surface of Mica Using Neutron Reflection. *The Journal of Physical Chemistry B* **2015,** *119* (21), 6457-6461.
51. Speranza, F.; Pilkington, G. A.; Dane, T. G.; Cresswell, P. T.; Li, P.; Jacobs, R. M. J.; Arnold, T.; Bouchenoire, L.; Thomas, R. K.; Briscoe, W. H., Quiescent bilayers at the mica-water interface. *Soft Matter* **2013,** *9* (29), 7028-7041.
52. Lamont, R. E.; Ducker, W. A., Surface-Induced Transformations for Surfactant Aggregates. *Journal of the American Chemical Society* **1998,** *120* (30), 7602-7607.
53. Kessel, A.; Ben-Tal, N.; May, S., Interactions of Cholesterol with Lipid Bilayers: The Preferred Configuration and Fluctuations. *Biophysical Journal* **2001,** *81* (2), 643-658.

54. Martín-Molina, A.; Rodríguez-Beas, C.; Faraudo, J., Effect of Calcium and Magnesium on Phosphatidylserine Membranes: Experiments and All-Atomic Simulations. *Biophysical Journal* **2012,** *102* (9), 2095-2103.
55. Martín-Molina, A.; Rodríguez-Beas, C.; Faraudo, J., Charge Reversal in Anionic Liposomes: Experimental Demonstration and Molecular Origin. *Physical Review Letters* **2010,** *104* (16), 168103.
56. Chen, C.-h.; Tian, C.-a.; Chiu, C.-c., The Effects of Alkyl Chain Combinations on the Structural and Mechanical Properties of Biomimetic Ion Pair Amphiphile Bilayers. *Bioengineering* **2017,** *4* (4).
57. Yang, J.; Appleyard, J., The Main Phase Transition of Mica-Supported Phosphatidylcholine Membranes. *The Journal of Physical Chemistry B* **2000,** *104* (34), 8097-8100.
58. Leonenko, Z. V.; Finot, E.; Ma, H.; Dahms, T. E. S.; Cramb, D. T., Investigation of temperature-induced phase transitions in DOPC and DPPC phospholipid bilayers using temperature-controlled scanning force microscopy. *Biophysical Journal* **2004,** *86* (6), 3783-3793.
59. Seeger, H. M.; Cerbo, A. D.; Alessandrini, A.; Facci, P., Supported Lipid Bilayers on Mica and Silicon Oxide: Comparison of the Main Phase Transition Behavior. *The Journal of Physical Chemistry B* **2010,** *114* (27), 8926-8933.
60. Gumí-Audenis, B.; Costa, L.; Ferrer-Tasies, L.; Ratera, I.; Ventosa, N.; Sanz, F.; Giannotti, M. I., Pulling lipid tubes from supported bilayers unveils the underlying substrate contribution to the membrane mechanics. *Nanoscale* **2018**.
61. Cevc, G.; Vierl, U., Nanotechnology and the transdermal route: A state of the art review and critical appraisal. *Journal of Controlled Release* **2010,** *141* (3), 277-299.
62. Proksch, R.; Schaffer, T. E.; Cleveland, J. P.; Callahan, R. C.; Viani, M. B., Finite optical spot size and position corrections in thermal spring constant calibration. *Nanotechnology* **2004,** *15* (9), 1344-1350.
63. Li, J. K.; Sullan, R. M. A.; Zou, S., Atomic Force Microscopy Force Mapping in the Study of Supported Lipid Bilayers. *Langmuir* **2011,** *27* (4), 1308-1313.
64. Phillips James, C.; Braun, R.; Wang, W.; Gumbart, J.; Tajkhorshid, E.; Villa, E.; Chipot, C.; Skeel Robert, D.; Kalé, L.; Schulten, K., Scalable molecular dynamics with NAMD. *Journal of Computational Chemistry* **2005,** *26* (16), 1781-1802.
65. Humphrey, W.; Dalke, A.; Schulten, K., VMD: Visual molecular dynamics. *Journal of Molecular Graphics* **1996,** *14* (1), 33-38.

TOC

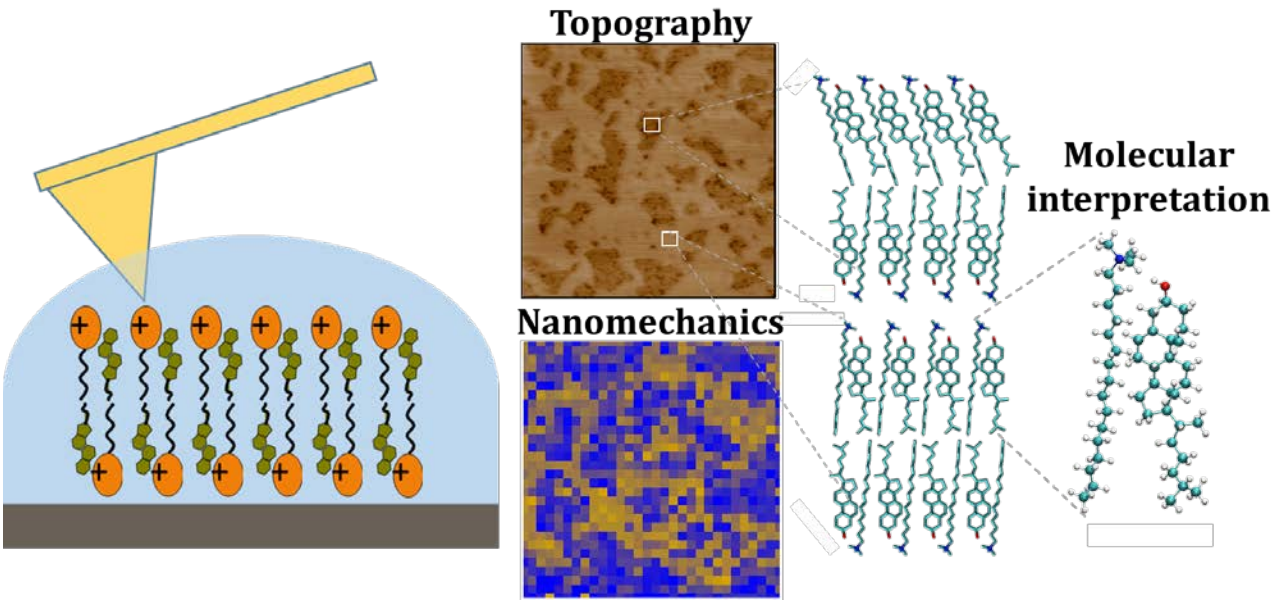
Topography
Nanomechanics
Molecular interpretation